

# DIAGNOSTIC TOOLS FOR MULTIFEED ARRAY ANTENNAS

Josef Migl<sup>1</sup>, Helmut Wolf<sup>1</sup>, Hans Steiner<sup>1</sup>, Rudolf Kis<sup>2</sup>

<sup>1</sup> Dornier Satellitensysteme GmbH (DSS) / Daimler-Benz-Aerospace,

P.O. Box 801169, 81663 Munich, Germany

<sup>2</sup> INTELSAT, Washington D.C., USA

## Abstract

Diagnostic tools for the determination of the excitation coefficients of a multifeed antenna based on pattern measurements are extremely useful during a spacecraft antenna design. Due to the complexity of state of the art multifeed antennas, it is not straightforward to isolate the location of possible error sources, if deficiencies or non-compliances are detected during an antenna measurement campaign.

Therefore a method was developed and tested at DSS which directly calculates the individual excitation coefficients of a multifeed array from pattern measurements.

The method approximates the measured composite array pattern by a set of computed element beam patterns, weighted by a set of unknown excitation coefficients. The resulting equation system is solved using the Method of Moments (MoM).

The tool has been extensively tested at DSS. The accuracy obtained for calculation of the coefficients was in the 2% range, which is comparable to the accuracy of Beam Forming Network (BFN) measurements using a network analyzer.

In this paper the theoretical background of the analysis methodology as well as some verification test cases will be described.

*Keywords: Antenna Measurements, Array Antennas, Excitation Coefficients, Method of Moments, Multifeed Antennas*

## 1. Introduction

Currently the excitation coefficients of multifeed antennas can only be measured at the Beam Forming Network (BFN) interface prior to the integration of the feed system and the antenna. Interactions with the feed elements (i.e., return loss, isolation of polarizers and mutual coupling between

feed elements) are not included. The accuracy of the effective excitation coefficients w.r.t. their design values can only be estimated by comparison between measured and predicted feed array patterns.

If parts of the BFN or feed elements are damaged during integration, qualification or transportation there is no direct way to determine which feed elements are affected or in which branch of the BFN the damage took place.

An important requirement for the diagnostic tool to be developed was that it can be used in any test range (i.e., far field, compact or near field test ranges). This is important since the installation and alignment of spacecraft antennas in the respective test facility is a time consuming task, therefore the re-installation in a tool specific range would be in conflict with continually decreasing schedules of space programs. Furthermore each transportation and re-installation of the antenna in another test facility constitutes an additional risk of damage and should be avoided.

In principle three major methods to solve the problem above can be considered:

1. Ray tracing based on geometrical optics (GO).
2. Imaging or holographic methods (i.e., transform near field data back to the feed array aperture).
3. Approximate the composite feed array pattern by a set of known element beam patterns and solve the equation system.

Ray tracing algorithms are not considered to be adequate, since ray tracing assumes that GO modeling of the antenna far-field radiation is sufficiently accurate. In the inverse case of the current problem, however (i.e., pattern prediction of a multifeed antenna from known excitation coefficients) the computation of multifeed patterns on a pure GO basis gives results far from the required accuracy.

Imaging methods are only applicable for near field (NF) test facilities. This theory, especially the numerical treatment method, is specifically tailored to the characteristics of NF test facilities (e.g., cylindrical, spherical or planar). This contradicts the objective of having a range independent tool. Furthermore the transformation of the NF to the aperture field of the feed

array is very CPU time intensive, and the calculation of the excitation coefficients from the global aperture field of the feed array is complicated and requires CPU time intensive modal expansion techniques. Again the inverse problem (i.e., the numerical efforts required to accurately compute the pattern of a multifeed system including mutual coupling effects) gives an indication of the numerical and computational efforts necessary to solve the current problem.

The third method is specifically tailored to the diagnostics of multifeed arrays and makes use of analysis tools required to solve the inverse problem (i.e., the computation of the multifeed pattern). This method is range independent, but assumes an accurate knowledge of the antenna, feed array and reflector geometry. This data is available from the antenna alignment measurements made in the test facility.

Another input for this method is the availability of analysis software to accurately predict the individual element beams including mutual coupling effects. This is not a major problem since the design of state of the art multifeed antennas with stringent isolation requirements can only be successfully optimized if such analysis tools are available.

For these reasons, the third method was selected to determine the excitation coefficients of multifeed antennas from pattern measurements of either the feed system or the complete antenna subsystem. The accuracy of the calculated excitation coefficients is a few tenth of a dB and a few degrees, which is within the measurement accuracy of the beam forming network (BFN) using a network analyzer.

## 2. Theory

The measured pattern  $\overset{p}{G}(u, v)$  on an arbitrary surface  $\Omega$  ( $\{u_i, v_j\} \in \Omega$ ), which is composed by the individual element pattern  $\overset{p}{G}_n(u, v)$ , weighted of the unknown excitation coefficients  $a_n$  in equation (1), is approximated by computed element pattern  $\overset{p}{G}_n^c(u, v)$  which are weighted by the unknown coefficients  $b_n$  in equation (2).

$$\overset{p}{G}(u, v) = \sum_{n=1}^N a_n \overset{p}{G}_n(u, v) \quad (1)$$

$$\overset{p}{G}(u, v) \approx \sum_{n=1}^N b_n \overset{p}{G}_n^c(u, v) \quad (2)$$

If the real element pattern is described by the computed element pattern with sufficient accuracy, a stationary behavior of the excitation coefficients may be assumed:

$$a_n \approx b_n. \quad (3)$$

The residue theorem [1]

$$\int_{\Omega} \overset{p}{R} \omega d\Omega = 0 \quad (4)$$

yields the arbitrary definition of the residue  $R$  as

$$\overset{p}{R} = \sum_{n=1}^N (a_n \overset{p}{G}_n^c(u, v)) - \overset{p}{G}(u, v) \quad (5)$$

to

$$\sum_{n=1}^N \int_{\Omega} a_n \overset{p}{G}_n^c(u, v) \omega d\Omega - \int_{\Omega} \overset{p}{G}(u, v) \omega d\Omega \approx 0. \quad (6)$$

If we now define the weighting function  $\omega$  as the complex conjugate pattern function

$$\omega = \overset{p}{G}_m^{c*}(u, v) = \overset{p}{G}_m^c(u, v); \quad m=1 \dots N \quad (7)$$

we get

$$\sum_{n=1}^N \left[ a_n \int_{\Omega} \overset{p}{G}_n^c(u, v) \cdot \overset{p}{G}_m^{c*}(u, v) d\Omega \right] - \int_{\Omega} \overset{p}{G}(u, v) \cdot \overset{p}{G}_m^{c*}(u, v) d\Omega \approx 0. \quad (8)$$

Applying the definition of the inner product

$$\langle \overset{p}{G}_n^c(u, v), \overset{p}{G}_m^{c*}(u, v) \rangle := \int_{\Omega} \overset{p}{G}_n^c(u, v) \cdot \overset{p}{G}_m^{c*}(u, v) d\Omega \quad (9)$$

to equation (8) we obtain the following approximation:

$$\langle \overset{p}{G}, \overset{p}{G}_m^c \rangle \approx \sum_{n=1}^N a_n \langle \overset{p}{G}_n^c, \overset{p}{G}_m^c \rangle. \quad (10)$$

Repeating this operation with each element pattern  $m = 1 \dots N$  yields the linear matrix equation

$$\begin{bmatrix} \langle \overset{p}{G}, \overset{p}{G}_1^c \rangle \\ \vdots \\ \langle \overset{p}{G}, \overset{p}{G}_N^c \rangle \end{bmatrix} \approx \begin{bmatrix} \langle \overset{p}{G}_1^c, \overset{p}{G}_1^c \rangle & \Lambda & \langle \overset{p}{G}_1^c, \overset{p}{G}_N^c \rangle \\ \vdots & \text{M} & \vdots \\ \langle \overset{p}{G}_N^c, \overset{p}{G}_1^c \rangle & \Lambda & \langle \overset{p}{G}_N^c, \overset{p}{G}_N^c \rangle \end{bmatrix} \cdot \begin{bmatrix} a_1 \\ \vdots \\ a_N \end{bmatrix} \quad (11)$$

which can be solved for the unknown excitation coefficients  $a$ .

## 3. Error Influence

Obviously one big unknown concerning the accuracy of the described method is the influence of errors in the computation of the element pattern, used as test and

weighting function, from the exact element pattern.

Another major problem is due to the fact that the composite beam pattern is measured at discrete sample points located on a finite section of a range dependent surrounding surface. Therefore the inner products in equation (9) have to be evaluated numerically, and the sampling rate of the measurement as well as the truncation of the measurement surface will influence the accuracy of the computation.

Finally error contributions due to measurement errors (e.g., noise, calibration errors, distortions from the test range etc.) also affect the accuracy of the computed excitation coefficients.

To investigate the influence of the above error contributions several calculations using analytical models have been prepared. A direct radiating planar array with rectangular aperture in a uniformly excited mode with 3x5 active elements served as one model. The geometrical parameters of the array are: Aperture size  $x=110$  mm,  $y=110$  mm, element spacing  $=111$  mm.

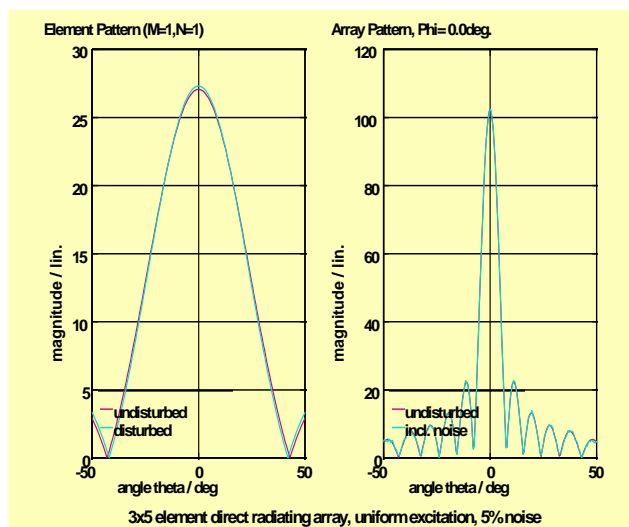


Figure 1: Simulation of a planar 3x5 element array, 10% error of test pattern, 5% noise signal

### 3.1 Influence of modeling accuracy of test and weighting functions

One of the major problems is the influence of errors on the test and weighting functions used to approximate the real

element patterns. Well proven and accurate analysis software for the computation of multifed antennas is a requirement for the described approach [2]. Differences of  $\pm 0.1$  dB at peak level and  $\pm 1$  dB at the  $-30$  dB level are typical values for deviations between computation and measurements, using multifed analysis software developed during INTELSAT R&D contracts.

To simulate the modeling errors of the computed element pattern from the real element pattern, a 10% referenced to the element pattern peak value was superposed on the element pattern, and a 5% noise level, referenced to the array peak, was overlaid on the array pattern (Figure 1).

The computed excitation coefficients of the planar array (Figure 1) compared to the exact excitation coefficients are shown in Figure 2. The errors are 0.025 dB and  $0.08^\circ$  at the  $-11.9$  dB level.

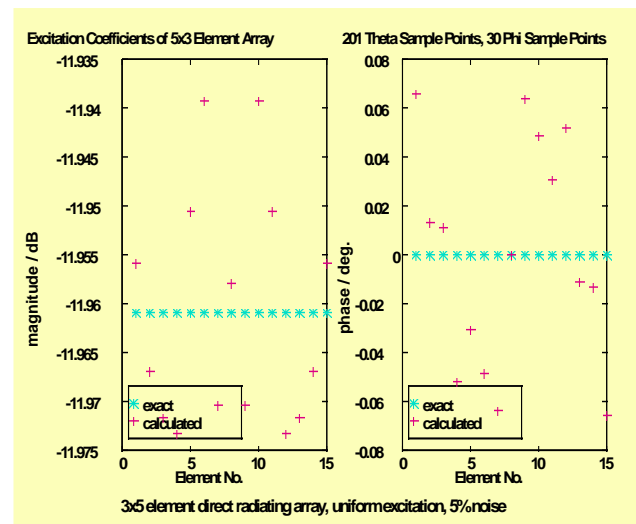


Figure 2: Exact and calculated excitation coefficients for uniformly excited direct radiating planar 3x5 element array

The results of the simulation of a reflector case (Figure 3) are shown in Figure 4. The simulation was performed for the mathematical model of a 3 m reflector with a focal length of 3 m. The reflector was illuminated by the planar 3x5 element array (Figure 1) used above. Again a good accuracy for the computed excitation coefficients was obtained, showing errors  $< 0.15$  dB and  $< 0.03^\circ$  at the  $-11.9$  dB level.

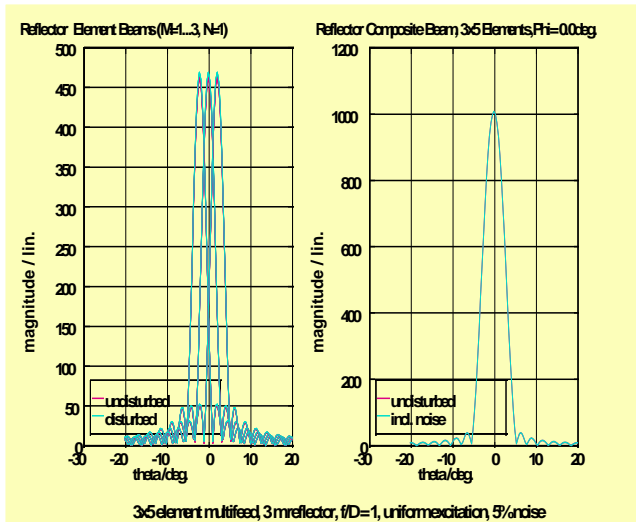


Figure 3: Pattern cuts of element beams and the composite beam of the planar 3x5 element array illuminating a reflector

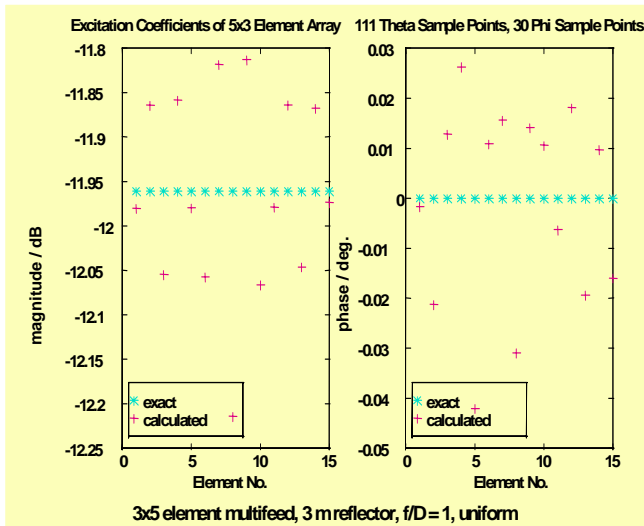


Figure 4: Exact and calculated excitation coefficients for uniformly excited planar 3x5 array illuminating a 3 m reflector

### 3.2 Truncation and sampling

All simulations performed showed sufficient convergence and accuracy if the measured pattern was sampled according to the Nyquist criterion. This is good practice for any conventional measurement, and therefore no additional requirements on the sampling rate are necessary for the proposed method.

Concerning the truncation of the measured field of view (FoV) the following rules of thumb seem to be valid:

1. Direct radiating array:  
The measurement FoV should, as a minimum, be the envelope of the main beams of all element patterns used as test and weighting functions.
2. Multifeed reflector:  
The measured FoV should, as a minimum, contain the main beam of the composite beam, i.e., the pattern of the reflector antenna.

Good accuracy is obtained, when the boundaries of the measurement FoV coincides with a nought of the respective reference beam.

### 4. Verification on Real Antenna Parameters

The INTELSAT VIII Hemi/Zone C-Band multifeed antenna (TX-module) was used to verify the tool on a real antenna design (Figure 5). The array consists of circular polarized (RHC) scrimp horns. For the verification only the elements of the Zone E were considered to be active. Nevertheless the design software takes into consideration mutual coupling effects between all active and passive elements.

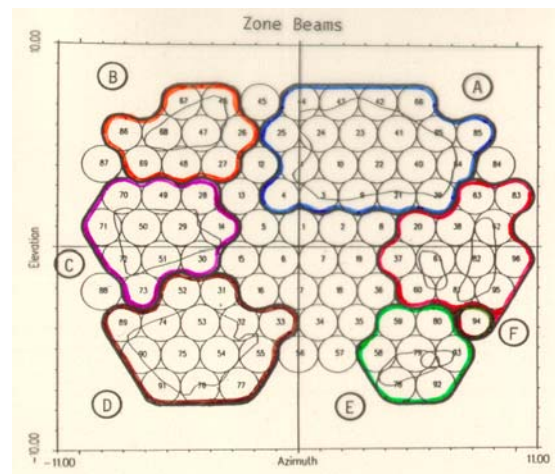


Figure 5: Schematic plot of the INTELSAT VIII Hemi/Zone TX antenna

The excitations of the antenna have been calculated in direct radiating and reflector scattering modes. Because of the synthetical origin of the data the simulation was done by adding errors to the composite array patterns.

Figure 6 shows the results for the ideal case. That means no errors were applied to the calculated element or composite array patterns. All calculated coefficients are almost identical and match the exact values within  $<0.03\text{dB}$  in magnitude and  $<0.0001^\circ$  in phase for the direct scattering

case. The results for the reflector radiating case show about the same magnitude of error.

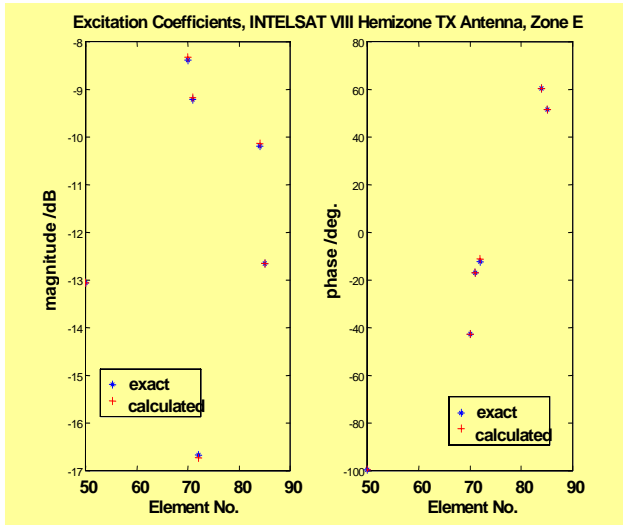


Figure 6: Exact and calculated excitation coefficients for the INTELSAT VIII Hemi/Zone TX antenna module in Zone E without any simulated error in direct radiation mode

The small deviations in the magnitude, are within expected numerical uncertainties, given the limited number of modes of the multimode feed horn used for the calculation of the element pattern and mutual coupling effects. In general, however, the results confirm the selected algorithm in the same manner as the simulation based on the planar array above.

In order to characterise the magnitude of errors due to typical antenna measurement uncertainties and design modeling accuracy some error cases are presented below.

Figure 7 shows the results for the direct radiating feed system. The following errors are added to the exact antenna pattern:

- TM01 mode with -25.0 dB level
- Axial ratio: -0.1dB
- Horn size (each): -0.5mm .

The worst deviation between exact and calculated excitation coefficients is 0.17dB in magnitude and 0.64° phase at approximately the -17dB level. The average values for this case are 0.055dB and 0.24°.

The excitation coefficients calculated with the same error contributions in a feed reflector arrangement are shown in Figure 8. The maximum error appears on element 72 with 0.12 dB magnitude and 0.85° phase at the -17dB level.

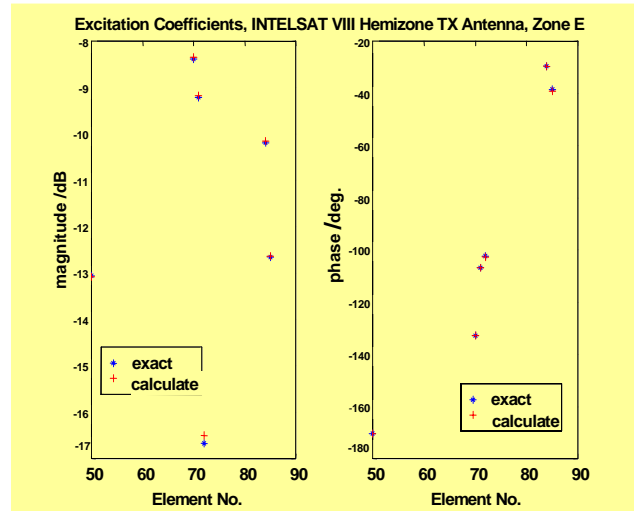


Figure 7: Exact and calculated excitation coefficients for the INTELSAT VIII Hemi/Zone TX antenna module in Zone E with simulated errors in direct radiation mode

The error parameter are: - axial ratio: -0.1dB  
 - TM01-mode: -25.0dB  
 element size: -0.5mm

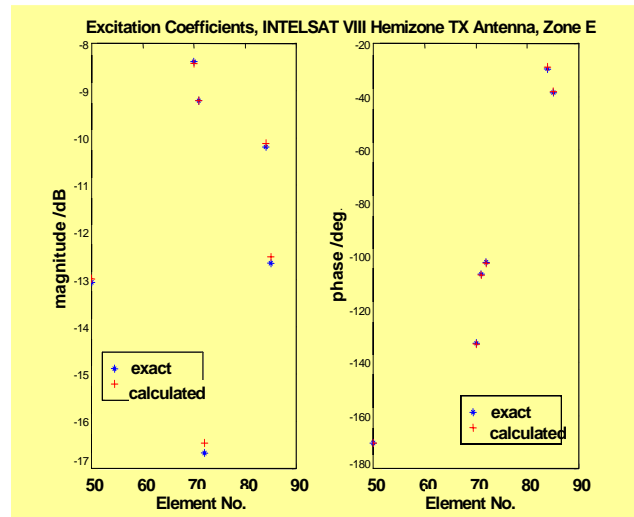


Figure 8: Exact and calculated excitation coefficients for the INTELSAT VIII Hemi/Zone TX antenna module in Zone E with simulated errors in reflector radiation mode

The error parameter are: - axial ratio: -0.1dB  
 - TM01-mode: -25.0dB  
 element size: -0.5mm

## 5. Conclusion

An analysis method has been presented for calculating the individual feed excitation coefficients of a multifeed array from pattern measurements. The method is range independent, flexible with respect to the antenna configuration, and CPU time efficient. In addition, results

obtained from the analytical investigations are very promising and confirm the accuracy of the proposed analysis method, even if the measurement signal is disturbed by considerable levels of noise or if the test and weighting pattern are loaded with considerable errors compared to the exact pattern. Although the results are not proofs in a strict mathematical sense, they do justify use of the selected analysis method.

Also, the analysis methodology selected (a) makes use of the discrete measurement data, avoiding the need for numerical integration, and (b) is relatively insensitive to sample rate and truncation of the measured field of view.

### **Acknowledgement**

This work is part of the ongoing INTELSAT study INTEL-1482 describing possibilities to improve the accuracy of antenna measurement ranges.

### **References**

- [1] Harrington, R.F., "Field Computation by Moment Methods", *Robert E. Krieger Publishing Company, Malabar, Florida*, pp. 5-21, Reprint 1982
- [2] Kühn, E., Wolf, H., Viskum, H., "Computer Analysis of Finite Planar Arrays of Circular Multimode Horns", *IEE Electronic Letters, Vol. 24, No. 18*, pp. 1150-1151, September 1988